Establishment and Mechanism Study of a Primary Ovarian Insufficiency Mouse Model using Lipopolysaccharide

Si-Ji Lv
Tongji University School of Medicine
Shu-Hui Hou
Tongji University School of Medicine
Lei Gan
Tongji University School of Medicine
Jing Sun (sunjing61867@tongji.edu.cn)
Tongji University School of Medicine

Research

Keywords: primary ovarian insufficiency, lipopolysaccharides, Cyclophosphamide, Inflammation, NF-kappa B

Posted Date: June 1st, 2021

DOI: https://doi.org/10.21203/rs.3.rs-545549/v1

Version of Record: A version of this preprint was published at Analytical Cellular Pathology on November 16th, 2021. See the published version at https://doi.org/10.1155/2021/1781532.

Abstract

Background: This study aimed to establish a lipopolysaccharide (LPS)-induced primary ovarian insufficiency (POI) mouse model and to investigate the underlying mechanism.

Methods: C57BL/6N female mice were intraperitoneally injected with low-dose LPS (0.5 mg/kg) once daily for 14 days, high-dose LPS (2.5 mg/kg) twice weekly for 2 weeks, and cyclophosphamide (CTX; 150 mg/kg) once weekly for 2 weeks. Ovarian function was assessed by measuring the length of the estrous cycle, the number of primordial follicles, and the levels of serum pituitary/ovarian hormones. Expression and production of interleukin 1β (IL-1β) were determined to evaluate ovarian inflammation. Histopathological examination was performed to examine ovarian fibrosis. TUNEL assay was carried out to evaluate granulosa cell apoptosis. Western blotting was performed to measure the levels of inflammation-, fibrosis-, and apoptosis-related proteins in mouse ovaries.

Results: Like CTX, both low- and high-dose LPS administration significantly impaired ovarian functions in mice, as evidenced by extended lengths of estrous cycles, reduced counts of primordial follicles, and alterations in the levels of serum hormones. Also, LPS administration promoted granulosa cell apoptosis and ovarian fibrosis in mice. However, LPS but not CTX significantly promoted IL-1β expression and production in mice. Moreover, LPS treatment but not CTX significantly enhanced TLR, p-p65, p65, and MyD88 protein expression in mouse ovaries, suggesting that LPS differs from CTX in triggering ovarian inflammation. In general, continuous low-dose LPS stimulation was less potent than high-dose LPS stimulation in the above-mentioned effects.

Conclusions: LPS induces ovarian inflammation, fibrosis, and granulosa cell apoptosis and can be used to establish a POI model in mice.

Background

Primary ovarian insufficiency (POI) is defined as the cessation of ovarian function before age 40 years, with an incidence of approximately 1% by age 40 and 0.1% by age 30. Patients with POI present menorrhoea, along with insufficient sex steroids such as estradiol (E2) and an increased follicle stimulating hormone (FSH) serum level (1). The etiologies of POI include genetic abnormalities (such as Turner syndrome and X-monosomy), autoimmunity, impaired metabolism (such as 17-OH deficiency and classic galactosaemia), exposure to radiation or chemotherapy, infections, as well as environmental pollutants and toxins(2–6). Since POI is a main cause of infertility in females (7, 8), a better understanding of its pathogenesis is necessary for the development of effective therapeutic strategies.

Owing to the similarity of the estrous cycles between female mice and humans, many studies have used POI mouse models to investigate the pathogenesis of POI and to develop therapeutic approaches(9–11). Chemotherapeutic drugs, like cyclophosphamide (CTX) and cisplatin, have been widely used to establish POI animal models due to their irreversible cytotoxicity toward ovaries, including destroying oocytes and arousing follicular depletion (12–14). Although chemotherapy is one of the potential etiologies for POI,

chemotherapeutic agent-induced POI may not simulate the pathophysiological condition of POI resulting from genetic, autoimmune, metabolic, and infectious factors (15). Thus, it is necessary to establish an animal model that simulates the complex pathogenic mechanisms underlying POI development.

Multiple mechanisms are involved in the development of POI, including ovarian inflammation, granulosa cell apoptosis, and ovarian fibrosis(16–18). A recent study has demonstrated that intraperitoneal (i.p.) administration of 0.5 mg/kg lipopolysaccharide (LPS) once daily for 6 days markedly reduces the sizes of the ovaries and uteri while increasing the number of preantral and atypical follicles of C57BL/6J mice. In addition, LPS treatment promotes protein expression of proinflammatory mediators in mouse ovaries, such as interleukin 1β (IL-1β), IL-18, toll-Like Receptor 4 (TLR4), and NOD-Like Receptor Family Pyrin Domain-Containing 3 (NLRP3). Moreover, NLRP3 activation facilitates ovarian fibrosis and granulosa cell pyroptotic death. These findings suggest that LPS treatment may cause POI and induce inflammation, granulosa cell death, and fibrosis in mouse ovaries (19). Thus, we hypothesized that LPS treatment can be applied to generate a POI animal model to investigate the development of POI and to find new therapeutic strategies.

To test our hypothesis, we treated C57BL/6N mice with low-dose LPS (0.5 mg/kg) for 14 consecutive days, high-dose LPS (2.5 mg/kg) twice weekly for 2 weeks, and CTX (150 mg/kg) once weekly for 2 weeks via i.p. injection to induce POI. We evaluated the effects of low- and high-dose LPS on ovarian function, inflammation, fibrosis, and granulosa cell apoptosis by comparing with those of CTX stimulation. Our results suggest LPS stimulation as a new method to establish a POI mouse model.

Results

LPS stimulation impairs ovarian function in mice.

To investigate whether LPS treatment could induce POI in mice, we examined estrous cycle length, primordial follicle counts, and pituitary/ovarian hormone serum levels in response to different doses of LPS. As shown in Fig. 1A, like CTX, both low- and high-dose LPS administration significantly extended the lengths of estrous cycles in mice compared with control. Although less potent than CTX, both low- and high-dose LPS administration remarkably reduced the counts of primordial follicles in mice compared with control (Fig. 1B). Furthermore, both high-dose LPS and CTX administration substantially reduced AMH and E2 serum levels while elevating FSH serum levels in mice. Low-dose LPS was less potent than high-dose LPS in reducing AMH and E2 serum levels and did not change FSH serum levels in mice (Fig. 1C). These changes are consistent with the characteristics of POI(1), suggesting that a 2-week stimulation with high-dose LPS twice weekly or low-dose LPS once daily induces POI in mice.

LPS stimulation induces ovarian inflammation in mice.

LPS is a potent inflammation trigger, and inflammation facilitates the development of POI(16, 22, 23). Figure 2A and 2B demonstrate that high- and low-dose LPS but not CTX significantly promoted IL-1β

expression and production in mice, suggesting that LPS but not CTX induces ovarian inflammation in mice.

LPS stimulation induces ovarian fibrosis in mice.

CTX stimulation causes ovarian fibrosis in mice(24). Masson staining revealed that like CTX, high-dose but not low-dose LPS resulted in significantly increased collagen deposition in mouse ovaries (Fig. 3A). qRT-PCR demonstrated that high-dose but not low-dose LPS treatment significantly upregulated Col1A1 mRNA expression in mouse ovaries (Fig. 3B). IHC staining showed that like CTX, both high- and low-dose LPS stimulation enhanced α-SMA protein expression in mouse ovaries (Fig. 3C). Consistently, WB result showed that low-dose LPS, high-dose LPS, and CTX upregulated protein expression of Col1A1and α-SMA (Fig. 3D). These findings suggest that like CTX, LPS induces interstitial fibrosis in mouse ovaries.

LPS stimulation promotes granulosa cell apoptosis in mouse ovaries.

Then, we examined cell apoptosis in mouse ovaries exposed to LPS treatment. As shown in Fig. 4A, TUNEL-positive granulosa cells were present in the ovaries of LPS- and CTX-treated mice. Moreover, LPS or CTX treatment significantly enhanced BAX both mRNA and protein expression while attenuating BCL-2 expression in mouse ovaries (Fig. 4B and 4C). These results suggest that like CTX, LPS treatment promotes granulosa cell apoptosis in mouse ovaries.

LPS activates TLR4/MyD88/NF-κB signaling in mouse ovaries.

Activation of LPS/TLR4/MyD88/NF-κB signaling promotes inflammation(25–27). Western blot analysis showed that compared with control, both low- and high-dose LPS treatments significantly enhanced TLR, p-p65, p65, and MyD88 protein expression in mouse ovaries, whereas CTX treatment attenuated the expression of these proteins (Fig. 5). Taken together, these data suggest that both LPS and CTX promotes ovarian fibrosis and granulosa cell apoptosis and that LPS differs from CTX in inducing ovarian inflammation.

Discussion

CTX causes POI due to ovarian cytotoxicity and is widely used to establish POI mouse models(24, 28). Although CTX has been shown to induce cortical fibrosis and follicle cell apoptosis that contribute to primordial follicle loss in POI mice(24), CTX stimulation is barely associated with inflammation that is a critical contributor to the etiology of POI(23). Here, we aimed to investigate whether the inflammation trigger LPS could induce POI in mice and to investigate the underlying mechanism. We demonstrated that

a 2-week stimulation with 2.5 mg/kg LPS twice weekly or 0.5 mg/kg LPS once daily induced POI in mice. Like CTX stimulation, LPS stimulation resulted in fibrosis and granulosa cell apoptosis in mouse ovaries. Importantly, LPS but not CTX induced ovarian inflammation in the POI mouse model, as evidenced by enhanced IL-1β expression and production as well as the activation of TLR/MyD88/NF-κB signaling in LPS-treated mice. These data suggest that in addition to ovarian fibrosis and follicle apoptosis, LPS also induces ovarian inflammation that is not achieved by CTX stimulation.

Bromfield et al. have reported that uterus or mammary gland infections with gram-negative bacteria cause infertility in cattle and that LPS exposure reduces the number of primordial follicles in the bovine ovarian cortex in vitro(29), suggesting that LPS may be used to establish POI animal models. By assessing the indicators of ovarian function, we found that like CTX, both low- and high-dose LPS administration resulted in significantly extended lengths of estrous cycles, decreased counts of primordial follicles, reduced levels of serum AMH and E2, as well as elevated levels of serum FSH in LPS-treated mice, consistent with the characteristics of POI (1). It appeared that low-dose LPS was less potent than high-dose LPS regarding these effects. These data suggest that we successfully establish an LPS-induced POI mouse model and that high-dose LPS stimulation outperforms continuous low-dose LPS stimulation in inducing POI in mice. Wang et al. have treated C57BL/6N mice with 0.5 mg/kg LPS once daily for 6 days or 5 mg/kg LPS once daily for 2 days and found that lose-dose LPS outperforms high-dose LPS in elevating the counts of preantral and atypical follicles and reducing the sizes of the ovaries and uteri(19). The different results between two studies are related to different LPS concentrations and treatment durations.

Inflammation contributes to the development of POI(22, 23). Patients with POI have significantly increased systemic inflammation indicator neutrophil-lymphocyte ratio (NLR) compared with healthy controls. The levels of serum FSH positively correlate with those of NLR in patients with POI(23). The anti-inflammatory drug can alleviate radiation-induced POI in rats by elevating AMH levels while reducing ovarian inflammation via inhibition of NF-κB provoked inflammatory cytokines(30). We found that LPS stimulation resulted in significantly enhanced IL-1β mRNA expression and secretion in mice compared with control. Consistently, Bromfield et al. have found that IL-1β, IL-6, and IL-8 are accumulated in bovine ovarian cortex culture supernatants in an LPS concentration-dependent manner(29). Wang et al. have shown that serum IL-1β levels are dramatically enhanced in high-dose LPS treated mice. Moreover, both low- and high-dose LPS treatments elevate serum IL-6 levels and enhance IL-1β and IL-18 protein expression in mouse ovaries(19). These findings collectively indicate that LPS induces ovarian inflammation.

LPS activates TLR4/NF-κB signaling to trigger inflammation(27, 31). Wang et al. have demonstrated that LPS treatment activates NF-κB signaling and promotes cell apoptosis of bovine ovarian granulosa cells, as evidenced by significantly increased p-p65 and caspase3 proteins levels as well as BAX/Bcl-2 ratios(32). Our Western blot analysis revealed that LPS stimulation significantly enhanced protein expression of TLR4, MyD88, BAX, and core components of NF-κB signaling while attenuating Bcl-2 expression in mouse ovaries, further confirming LPS promotes NF-κB signaling and cell apoptosis in

mouse ovaries. Importantly, the alterations in inflammation-related protein expression were negligible in CTX-treated mice, suggesting that LPS but not CTX triggers ovarian inflammation in mice. Furthermore, LPS treatment exhibited similar or more potent effects on the upregulation of Col1A1 and α-SMA protein expression, suggesting that LPS is at least comparable to CTX in inducing ovarian fibrosis.

Conclusions

In conclusion, we successfully established an LPS-induced POI mouse model and demonstrated that LPS stimulation not only induced fibrosis and granulosa cell apoptosis but also triggered inflammation that is not achieved by CTX stimulation in mouse ovaries. These results suggest LPS stimulation as a new strategy to establish POI mouse models for the investigation of the complex etiology of POI.

Methods

Animals

This study was approved by the Ethics Committee of Tongji University (#TJBG03621101; Shanghai, China) and carried out following the Guide for the Care and Use of Laboratory Animals of Tongji University. A total of 40 C57BL/6N female mice (6–8-week old; Beijing Vital River Laboratory Animal Technology, China) were maintained at the Animal Research Center of Tongji University under a 12/12-h light/dark cycle with free access to water and food.

POI mouse model

Mice were randomly assigned to control, low-dose LPS, high-dose LPS, and CTX groups (n = 10/group). To induce POI, mice were administered 0.5 mg/kg LPS (L2630; Sigma-Aldrich, St. Louis, MO, USA) once daily for 14 days, 2.5 mg/kg LPS twice weekly for 2 weeks, or 150 mg/kg CTX (C0768; Sigma-Aldrich) once weekly for 2 weeks via i.p. injection. At 2 weeks after treatment, mice were anesthetized with 1% sodium pentobarbital via i.p. injection, followed by blood sample collection through cardiac puncture. After cervical dislocation, the ovaries were immediately collected and fixed with 4% paraformaldehyde or stored at − 80°C until use.

Monitoring the estrous cycle

The vaginal epithelial cells were collected daily by vaginal lavage to monitor the estrous cycle. Cells were observed using a light microscope (Eclipse E100; Nikon, Japan) under the bright field. Images were acquired at 10× magnification using a Nikon DS-U3 imaging system. Representative cell morphologies at corresponding cycle phases are shown in **Supplementary Fig. 1**.

Histopathological examination

The ovary tissue samples were fixed in 4% paraformaldehyde overnight, dehydrated, paraffin-embedded, and sliced into 4-μm-thick sections. After dewaxing and rehydration, the sections were subjected to hematoxylin & eosin (H&E), immunohistochemical (IHC), or Masson staining following standard

methods. H&E staining was performed to count primordial follicles as previously described(20). For each mouse, the primordial follicles in three consecutive sections were counted. For IHC staining, the sections were immersed in sodium citrate solution (0.01 M) for 20–30 min for antigen retrieval, followed by incubation with 3% hydrogen peroxide to quench the endogenous peroxidase. Then, the section was blocked with 3% bovine serum albumin (BSA) for 30 min at room temperature, followed by an overnight incubation with primary anti-α-smooth muscle actin (α-SMA) antibody (Servicebio, Wuhan, Hubei, China) at 4 ºC and phosphate buffered saline (PBS) rinses. After an incubation with the secondary antibody for 50 min at room temperature, the section was stained using a DAB detection kit (DAKO, Agilent Technologies, Santa Clara, CA, USA). Images were acquired using an XSP-C204 microscope (COIC, Chongqing, China). The results were assessed by two independent pathologists in a blinded manner. The intensity of the staining was scored as previously described(21). For Masson staining, the collagen fibers in ovarian tissue samples were stained using a Masson staining kit (Guge Biotechnology, Wuhan, Hubei, China). The blue-stained collagen fibers were observed using an optical microscopy (DS-U3; Nikon, Japan) at magnification 10×. The Masson-positive area was quantified using Image J v1.8.0 (NIH, Bethesda, MD, USA).

TUNEL assay

Ovarian granulosa cell apoptosis was examined using a TUNEL assay kit (Servicebio). Briefly, deparaffinized sections were incubated with 20 mg/mL proteinase K (Guge Biotechnology) at 37°C for 20 min, followed by incubation with permeabilization buffer at room temperature for 20 min. After a 10-min equilibration at room temperature, sections were incubated with terminal deoxynucleotidyl transferase and deoxyuridine triphosphate at 37°C for 2 h in a moist chamber. Images were acquired using a Nikon Eclipse Ti-SR microscope.

Enzyme-linked immunosorbent assay (ELISA)

The serum levels of anti-Müllerian hormone (AMH), E2, FSH, and IL-1β were measured using the corresponding ELISA kit (Elabscience, Wuhan, Hubei, China) following the manufacturer’s protocols.

Quantitative real-time PCR (qRT-PCR)

Total RNA was isolated from ovarian tissue samples using Trizol (RNAiso Plus; Takara, Japan). cDNA was synthesized using a PrimeScript™ RT reagent kit (Takara). Amplification was performed using TB Green® Premix EX TaqTM II (Takara) and gene-specific primers (Table 1; Sangon, Shanghai, China) on a qRT-PCR device (QuantStudio5, Thermo Fisher Scientific, Waltham, MA, USA). The relative mRNA levels of the genes were quantified using the $2^{-\Delta\Delta CT}$ method and normalized to GAPDH mRNA level.

Table 1
Primers for quantitative real-time PCR.

Gene	Forward (5'–3')	Reverse (5'–3')
GAPDH	GACTGGATAAGCAGGGCGG	CCCAATACGGCCAAATCCGT
IL-1β	GAAATGCCACCTTTTGACAGTG	CTGGATGCTCTCATCAGGACA
COL1A1	TGACCTTCCTGCGCCTAATG	AAGTTCCGGTGTGACTCGTG
BAX	GGCCTTTTTGCTACAGGGTTTC	CAGCTTCTTGGTGGACGCAT
BCL-2	GCTGGGTAGGTGCATGTCTG	CAGGGGAGCAAAGCTACAAACT

Western blot analysis

The ground ovarian tissue samples were lysed using RIPA buffer (Biotechwell, Shanghai, China). Total proteins were isolated by centrifuging the lysates at 12,000 rpm for 5 min. Protein concentrations were measured using a bicinchoninic acid kit (Biotechwell). The proteins were separated using gel electrophoresis and then transferred to a polyvinylidene fluoride membrane. The membrane was blocked using 5% BSA for 2 h at room temperature, followed by an overnight incubation with anti-TLR (1:1000; Cell Signaling Technology, Danvers, MA, USA), anti-Bcl-2 (1:1000; Affinity, Scoresby, Victoria, Australia), anti-collagen type I alpha 1 chain (Col1A1; 1:1000; Affinity), anti-α-SMA (1:1500; Servicebi), anti-BAX (1:1500; ImmunoWay Biotechnology, Plano, TX, USA), anti-P-P65 (1:1000; ImmunoWay Biotechnology), anti-MyD88 (1:1000; ImmunoWay Biotechnolog), anti-P65 (1:1000; Affinity), or anti-GAPDH (1:2000; Biotechwell) at 4°C. After a 2-h incubation with a secondary antibody (1:2000; Jackson Immuno, West Grove, PA, USA) at room temperature, the protein bands were developed using an enhanced chemiluminescence kit (Biotechwell).

Statistical analysis

Data were presented as the mean ± standard error of the mean. Statistical analysis was carried out using the SPSS software (V18.0; IBM, Armonk, NY, USA). Intergroup differences were compared using one-way analysis of variance. Statistical significance was analyzed using the Student's *t*-test. A *P* value less than 0.05 was considered statistically significant.

Abbreviations

α-SMA	anti-α-smooth muscle actin
BSA	bovine serum albumin
ELISA	Enzyme-linked immunosorbent assay
FSH	follicle stimulating hormone
H&E	hematoxylin & eosin
IHC	immunohistochemical
LPS	lipopolysaccharide
NLR	neutrophil-lymphocyte ratio
NLRP3	NOD-Like Receptor Family Pyrin Domain-Containing 3
PBS	phosphate buffered saline
POI	primary ovarian insufficiency
qRT-PCR	Quantitative real-time PCR
TLR4	toll-Like Receptor 4

Declarations

Ethics approval and consent to participate

The animal study was approved by the Ethics Committee of Tongji University (#TJBG03621101; Shanghai, China). All experiments were performed following the Guide for the Care and Use of Laboratory Animals of Tongji University.

Consent for publication

Not applicable.

Availability of data and materials

The datasets used and/or analysed during the current study are available from the corresponding author on reasonable request.

Competing interests

The authors declare no conflicts of interest.

Funding

This study was financially supported by Clinical Technology Innovation Project of Shanghai Shenkang Hospital Development Center (Grant No. SHDC12019113); Advanced Appropriate Technology Promotion Project of Shanghai Health Commission (Grant No. 2019SY002); Scientific Research Project of Shanghai Science and Technology Commission (Grant No. 19411960300).

Authors' contributions

Si-Ji Lv carried out the studies, participated in collecting data, and drafted the manuscript. Shu-Hui Hou participated in its design. Lei Gan contributed reagents and analytic tools. All authors read and approved the final manuscript.

Acknowledgments

The authors would like to thank all study participants who were enrolled in this study.

References

1. Jankowska K. Premature ovarian failure. Prz Menopauzalny. 2017;16:51-6.
2. Rudnicka E, Kruszewska J, Klicka K, Kowalczyk J, Grymowicz M, Skorska J, et al. Premature ovarian insufficiency - aetiopathology, epidemiology, and diagnostic evaluation. Prz Menopauzalny. 2018;17:105-8.
3. Rossetti R, Ferrari I, Bonomi M, Persani L. Genetics of primary ovarian insufficiency. Clin Genet. 2017;91:183-98.
4. Kirshenbaum M, Orvieto R. Premature ovarian insufficiency (POI) and autoimmunity-an update appraisal. J Assist Reprod Genet. 2019;36:2207-15.
5. Abidin Z, Treacy EP. Insights into the Pathophysiology of Infertility in Females with Classical Galactosaemia. Int J Mol Sci. 2019;20.
6. Lambertini M, Moore HCF, Leonard RCF, Loibl S, Munster P, Bruzzone M, et al. Gonadotropin-Releasing Hormone Agonists During Chemotherapy for Preservation of Ovarian Function and Fertility in Premenopausal Patients With Early Breast Cancer: A Systematic Review and Meta-Analysis of Individual Patient-Level Data. J Clin Oncol. 2018;36:1981-90.
7. Walker MH, Tobler KJ. Female Infertility. StatPearls. Treasure Island (FL)2021.
8. Chapman C, Cree L, Shelling AN. The genetics of premature ovarian failure: current perspectives. Int J Womens Health. 2015;7:799-810.
9. Liu TE, Wang S, Zhang L, Guo L, Yu Z, Chen C, et al. Growth hormone treatment of premature ovarian failure in a mouse model via stimulation of the Notch-1 signaling pathway. Exp Ther Med.

2016;12:215-21.

10. Zhang J, Fang L, Shi L, Lai Z, Lu Z, Xiong J, et al. Protective effects and mechanisms investigation of Kuntai capsule on the ovarian function of a novel model with accelerated aging ovaries. J Ethnopharmacol. 2017;195:173-81.
11. He L, Ling L, Wei T, Wang Y, Xiong Z. Ginsenoside Rg1 improves fertility and reduces ovarian pathological damages in premature ovarian failure model of mice. Exp Biol Med (Maywood). 2017;242:683-91.
12. Fu X, He Y, Wang X, Peng D, Chen X, Li X, et al. Overexpression of miR-21 in stem cells improves ovarian structure and function in rats with chemotherapy-induced ovarian damage by targeting PDCD4 and PTEN to inhibit granulosa cell apoptosis. Stem Cell Res Ther. 2017;8:187.
13. Li J, Yu Q, Huang H, Deng W, Cao X, Adu-Frimpong M, et al. Human chorionic plate-derived mesenchymal stem cells transplantation restores ovarian function in a chemotherapy-induced mouse model of premature ovarian failure. Stem Cell Res Ther. 2018;9:81.
14. Luan Y, Edmonds ME, Woodruff TK, Kim SY. Inhibitors of apoptosis protect the ovarian reserve from cyclophosphamide. J Endocrinol. 2019;240:243-56.
15. Torrealday S, Kodaman P, Pal L. Premature Ovarian Insufficiency - an update on recent advances in understanding and management. F1000Res. 2017;6:2069.
16. Chen H, Xiao X, Shan D, Li W, Liao Y, Xu L. Platelet-activating factor acetylhydrolase and premature ovarian failure. Clin Exp Obstet Gynecol. 2014;41:613-6.
17. Ford JH. Reduced quality and accelerated follicle loss with female reproductive aging - does decline in theca dehydroepiandrosterone (DHEA) underlie the problem? J Biomed Sci. 2013;20:93.
18. Erbas O, Pala HG, Pala EE, Oltulu F, Aktug H, Yavasoglu A, et al. Ovarian failure in diabetic rat model: nuclear factor-kappaB, oxidative stress, and pentraxin-3. Taiwan J Obstet Gynecol. 2014;53:498-503.
19. Wang C, Horby PW, Hayden FG, Gao GF. A novel coronavirus outbreak of global health concern. Lancet. 2020;395:470-3.
20. Nie X, Dai Y, Zheng Y, Bao D, Chen Q, Yin Y, et al. Establishment of a Mouse Model of Premature Ovarian Failure Using Consecutive Superovulation. Cell Physiol Biochem. 2018;51:2341-58.
21. Levan K, Mehryar M, Mateoiu C, Albertsson P, Back T, Sundfeldt K. Immunohistochemical evaluation of epithelial ovarian carcinomas identifies three different expression patterns of the MX35 antigen, NaPi2b. BMC Cancer. 2017;17:303.
22. Huang Y, Hu C, Ye H, Luo R, Fu X, Li X, et al. Inflamm-Aging: A New Mechanism Affecting Premature Ovarian Insufficiency. J Immunol Res. 2019;2019:8069898.
23. Agacayak E, Yaman Goruk N, Kusen H, Yaman Tunc S, Basaranoglu S, Icen MS, et al. Role of inflammation and oxidative stress in the etiology of primary ovarian insufficiency. Turk J Obstet Gynecol. 2016;13:109-15.
24. Chen XY, Xia HX, Guan HY, Li B, Zhang W. Follicle Loss and Apoptosis in Cyclophosphamide-Treated Mice: What's the Matter? Int J Mol Sci. 2016;17.

25. Ju M, Liu B, He H, Gu Z, Liu Y, Su Y, et al. MicroRNA-27a alleviates LPS-induced acute lung injury in mice via inhibiting in fl ammation and apoptosis through modulating TLR4/MyD88/NF-kappaB pathway. Cell Cycle. 2018;17:2001-18.
26. Hu N, Wang C, Dai X, Zhou M, Gong L, Yu L, et al. Phillygenin inhibits LPS-induced activation and inflammation of LX2 cells by TLR4/MyD88/NF-kappaB signaling pathway. J Ethnopharmacol. 2020;248:112361.
27. Kawai T, Takeuchi O, Fujita T, Inoue J, Muhlradt PF, Sato S, et al. Lipopolysaccharide stimulates the MyD88-independent pathway and results in activation of IFN-regulatory factor 3 and the expression of a subset of lipopolysaccharide-inducible genes. J Immunol. 2001;167:5887-94.
28. Elkady MA, Shalaby S, Fathi F, El-Mandouh S. Effects of quercetin and rosuvastatin each alone or in combination on cyclophosphamide-induced premature ovarian failure in female albino mice. Hum Exp Toxicol. 2019;38:1283-95.
29. Bromfield JJ, Sheldon IM. Lipopolysaccharide reduces the primordial follicle pool in the bovine ovarian cortex ex vivo and in the murine ovary in vivo. Biol Reprod. 2013;88:98.
30. Said RS, El-Demerdash E, Nada AS, Kamal MM. Resveratrol inhibits inflammatory signaling implicated in ionizing radiation-induced premature ovarian failure through antagonistic crosstalk between silencing information regulator 1 (SIRT1) and poly(ADP-ribose) polymerase 1 (PARP-1). Biochem Pharmacol. 2016;103:140-50.
31. Cheng P, Wang T, Li W, Muhammad I, Wang H, Sun X, et al. Baicalin Alleviates Lipopolysaccharide-Induced Liver Inflammation in Chicken by Suppressing TLR4-Mediated NF-kappaB Pathway. Front Pharmacol. 2017;8:547.
32. Wang X, Li C, Wang Y, Li L, Han Z, Wang G. UFL1 Alleviates LPS-Induced Apoptosis by Regulating the NF-kappaB Signaling Pathway in Bovine Ovarian Granulosa Cells. Biomolecules. 2020;10.

Figures

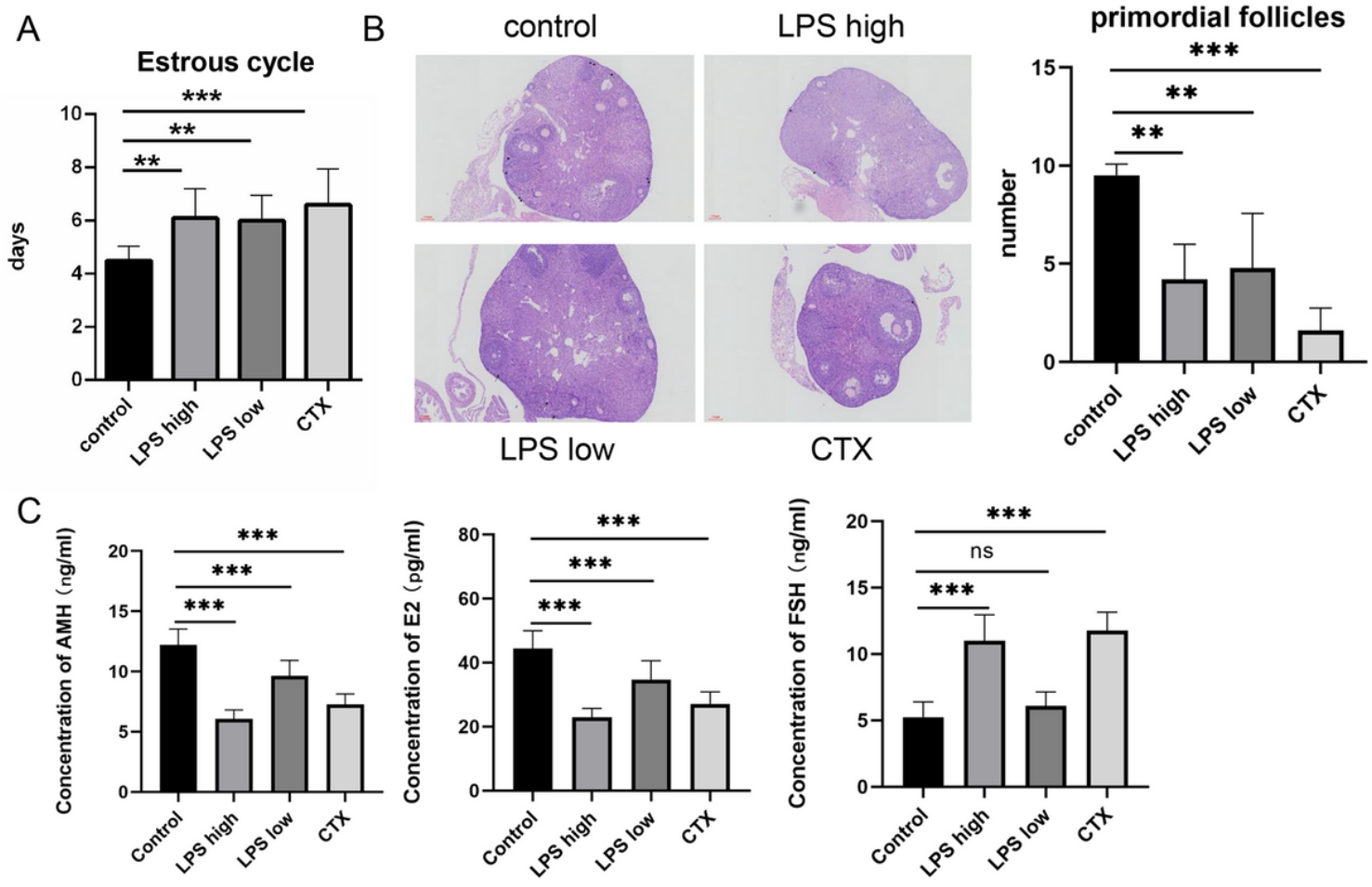

Figure 1

Lipopolysaccharide (LPS) induced ovarian dysfunction in mice. C57BL/6N female mice (6 to 8-week-old) were administered control, low-dose LPS (0.5 mg/kg once daily), high-dose LPS (2.5 mg/kg twice weekly), or cyclophosphamide (CTX; 150 mg/kg once weekly) for 2 weeks via intraperitoneal injection. (A) The lengths of estrous cycles were determined by daily observations of vaginal epithelial cell cytology. (B) Hematoxylin & eosin staining was performed to count primordial follicles (black arrow). Scale bar: 100μm. (C) Enzyme-linked immunosorbent assay (ELISA) was conducted to measure serum levels of AMH, E2, and FSH at 2 weeks after treatment. Data are expressed as the mean ± standard error of the mean (SEM). **P < 0.01, ***P < 0.001; ns, non-significant; n = 10. AMH: anti-Müllerian hormone; E2: estradiol; FSH: follicle stimulating hormone.

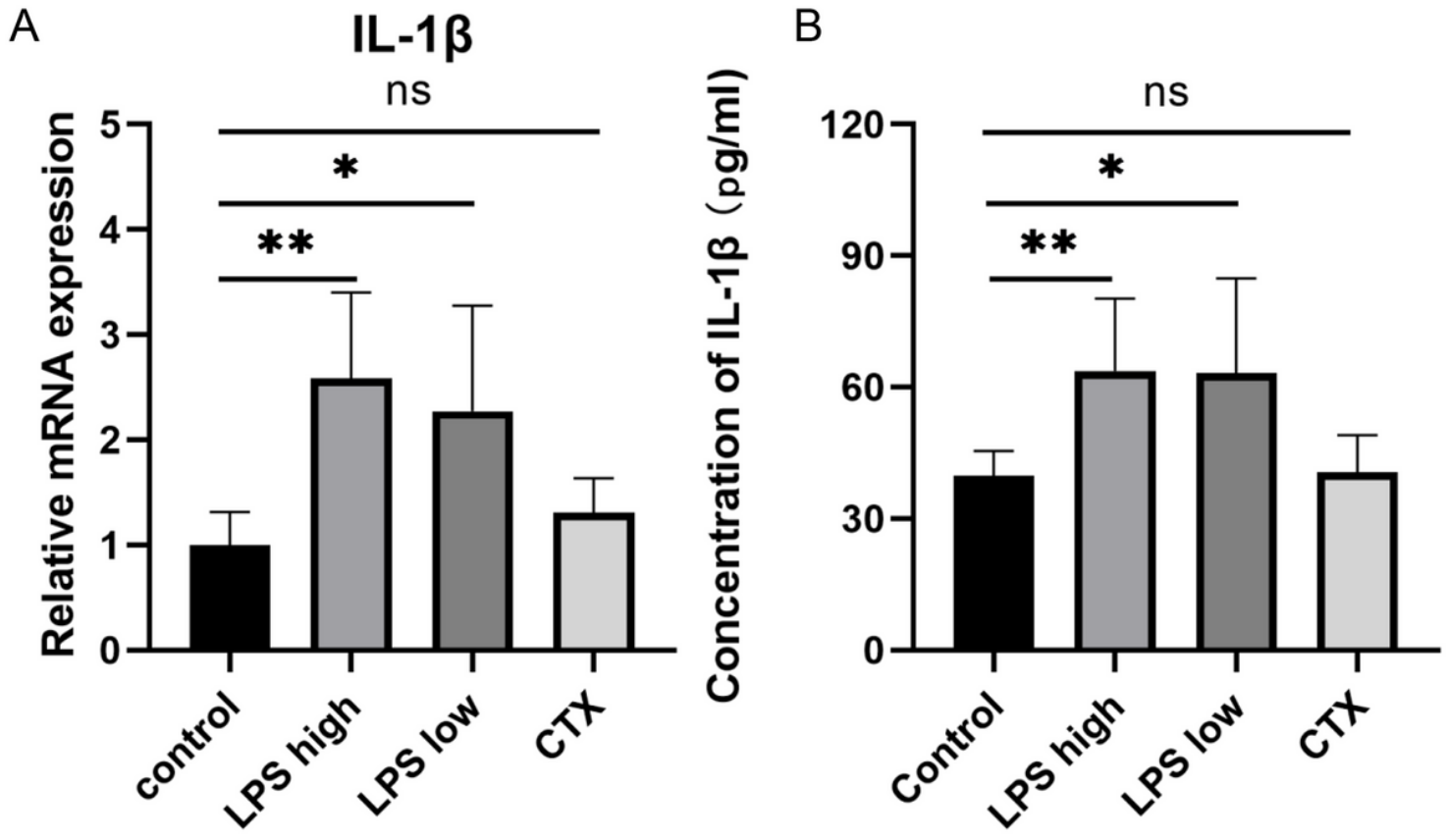

Figure 2

LPS stimulation promoted interleukin 1β (IL-1β) expression and production in mice. Mice were sacrificed at 2 weeks after LPS or CTX treatment. (A) Quantitative real-time PCR (qRT-PCR) was conducted to measure IL-1β mRNA expression in mouse ovary tissue samples. (B) ELISA was conducted to measure IL-1β serum levels in mice. Data are expressed as the mean ± SEM. *P < 0.05, **P < 0.01; ns, non-significant, n = 10.

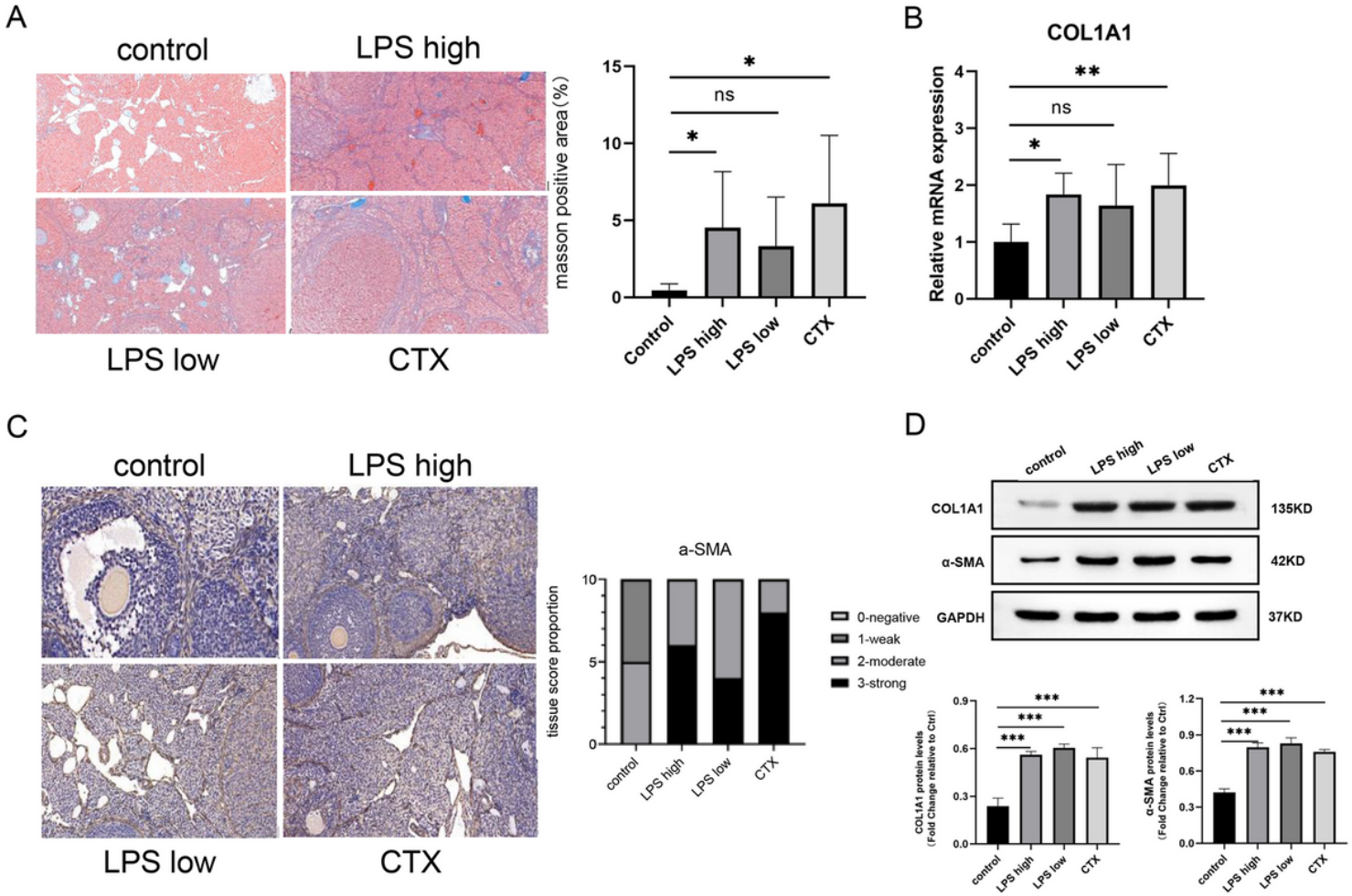

Figure 3

LPS stimulation induced ovarian fibrosis in mice. (A) Masson staining was performed to detect collagen deposition in mouse ovaries. Representative images are shown. Scale bar: 100μm. (B) qRT-PCR was performed to measure Col1A1 mRNA expression in mouse ovaries. (C) Immunohistochemical staining was carried out to detect α-SMA expression in mouse ovaries. Representative images are shown. Scale bar: 100μm. (D) Western blot analysis was carried out to measure Col1A1 and α-SMA protein expression in mouse ovaries. Data are expressed as the mean ± SEM. *P < 0.05, **P < 0.01; ***P < 0.001, n = 10. Col1A1: type I procollagen; α-SMA: α-smooth muscle actin.

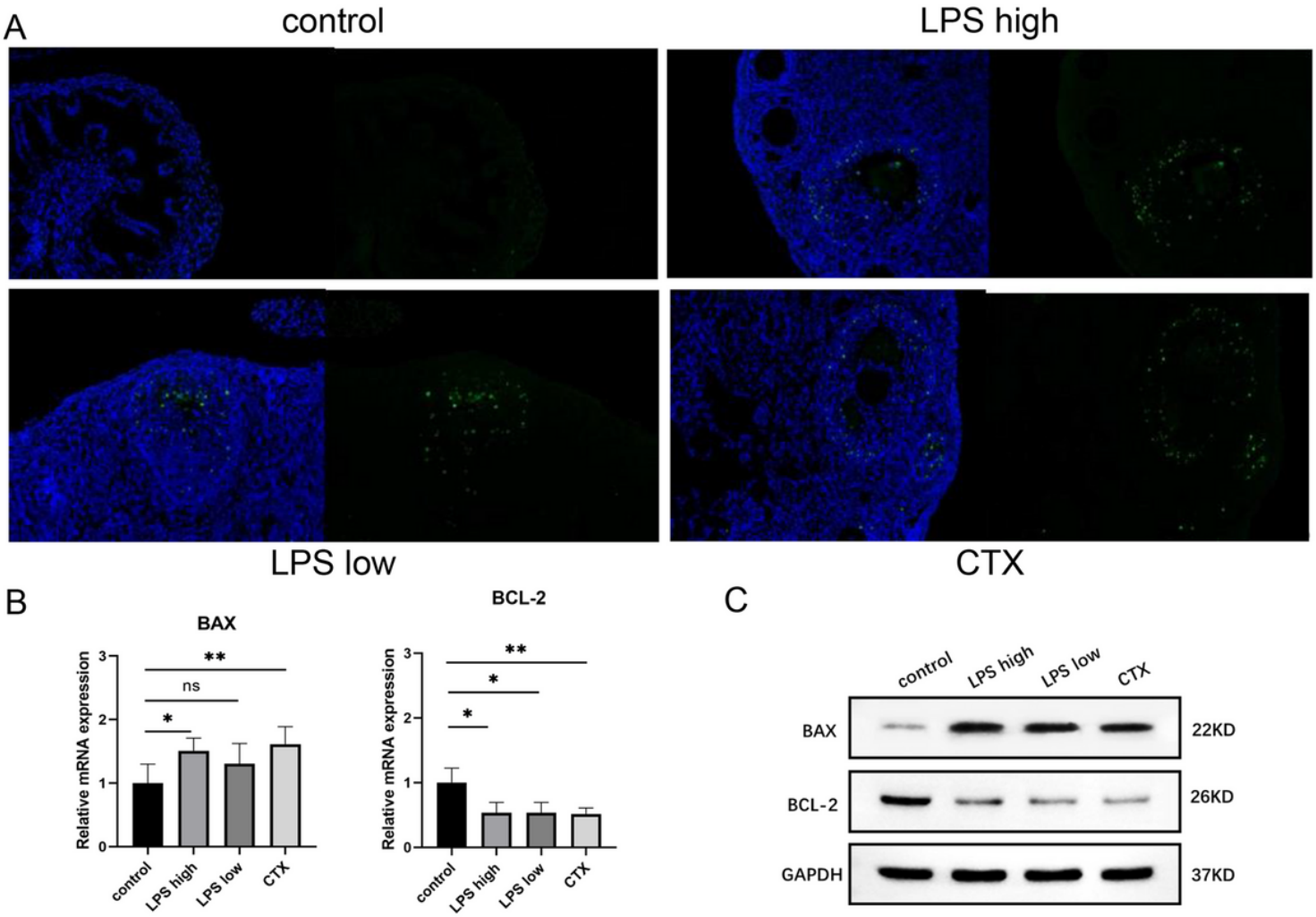

Figure 4

LPS stimulation induced granulosa cell apoptosis in mouse ovaries. (A) TUNEL assay was performed to examine granulosa cell apoptosis. Representative images are shown, blue represents nuclear, green represents apoptosis granule. Magnification 10×. (B) qRT-PCR and (C) Western blot analysis was performed to measure mRNA and protein expression of BAX and BCL2 in mouse ovaries. Data are expressed as the mean ± SEM. *P < 0.05, **P < 0.01; ns, non-significant; n = 10.

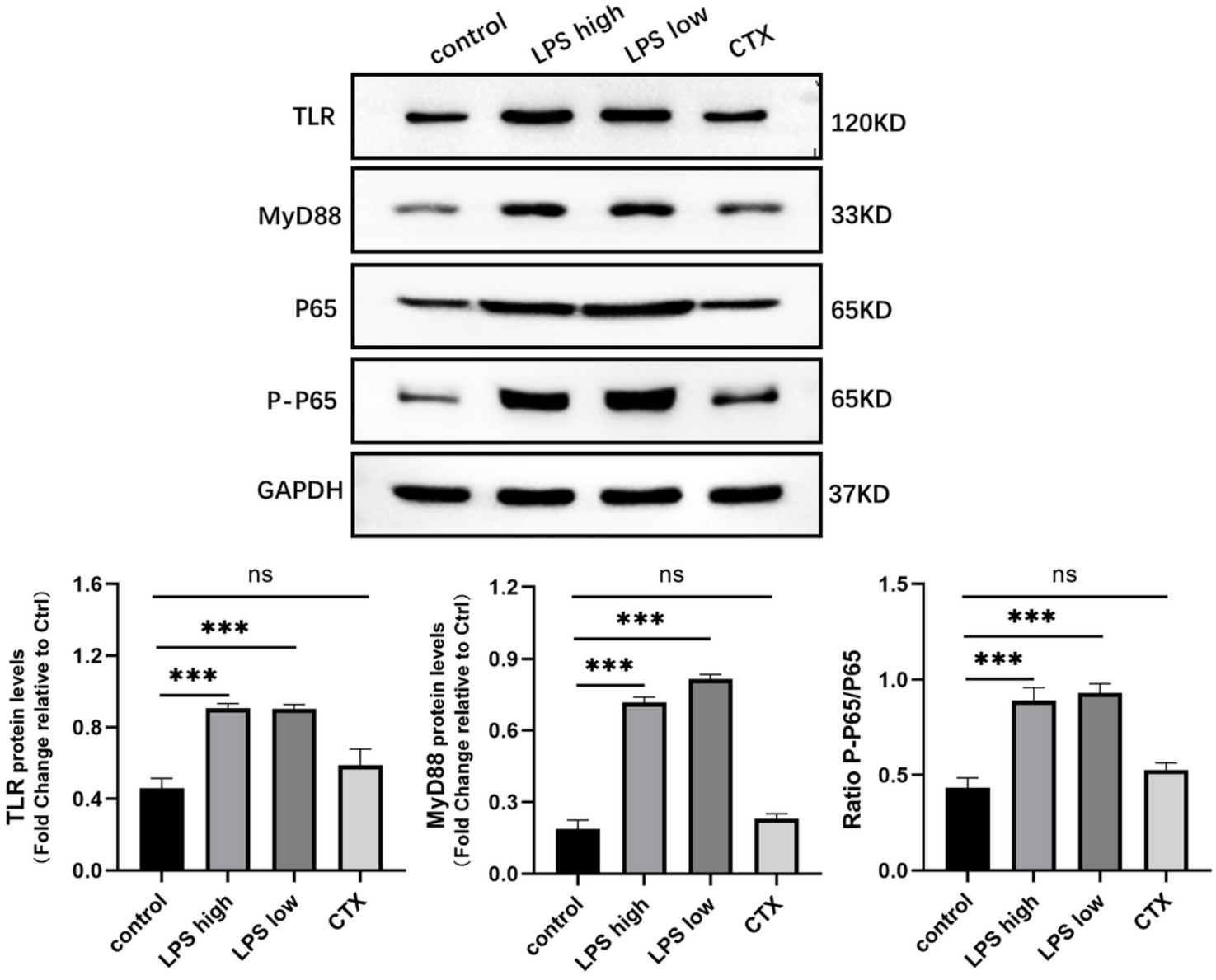

Figure 5

The expression of inflammationrelated proteins. Western blot analysis was performed to measure protein expression of TLR, MyD88, P-P65, P-65, or GAPDH in mouse ovaries. Data are expressed as the mean ± SEM. ***P < 0.001, ns, non-significant.

Supplementary Files

This is a list of supplementary files associated with this preprint. Click to download.

- SupplementaryFigure1.tif